Hindawi Publishing Corporation
Advances in Chemistry
Volume 2014, Article ID 490358, 5 pages
http://dx.doi.org/10.1155/2014/490358

Research Article

Structural Conformational Study of Eugenol Derivatives Using Semiempirical Methods

Radia Mahboub

Department of Chemistry, Faculty of Sciences, University of Tlemcen, BP 119, 13000 Tlemcen, Algeria

Correspondence should be addressed to Radia Mahboub; radiamahboub@yahoo.com

Received 3 June 2014; Accepted 29 September 2014; Published 20 October 2014

Academic Editor: Maria Roca

We investigated the conformational structure of eugenol and eugenyl acetate under torsional angle effect by performing semiempirical calculations using AM1 and PM3 methods. From these calculations, we have evaluated the strain energy of conformational interconversion. To provide a better estimate of stable conformations, we have plotted the strain energy versus dihedral angle. So, we have determined five geometries of eugenol (three energy minima and two transition states) and three geometries of eugenyl acetate (two energy minima and one transition state). From the molecular orbital calculations, we deduce that the optimized *trans* form by AM1 method is more reactive than under PM3 method. We can conclude that both methods are efficient. The AM1 method allows us to determine the reactivity and PM3 method to verify the stability.

1. Introduction

Eugenol (4-allyl-2-methoxyphenol) is a phenylpropene, an allyl chain-substituted guaiacol. It is the main phenolic compound extracted from certain essential oils especially from clove oil, nutmeg, cinnamon, basil, and bay leaf [1–14]. Eugenol is a phenol derivative used in many areas such as perfumes, flavorings agent, and dental materials. It is used as an antiseptic, analgesic, fungicide, bactericide, insecticide, anticarcinogenic, antiallergic, antioxidant, anti-inflammatory, and so forth [15–17]. As derivative, the eugenyl acetate was characterized and its structural properties have investigated by Dos Santos et al. [18, 19].

To our knowledge, a study of the conformational structure as a function of the dihedral angle was not reported. In the present paper, we investigated the conformational structure of eugenol and eugenyl acetate under torsional angle effect by performing semiempirical calculations using AM1 and PM3 methods. From these calculations, we have evaluated the strain energy of conformational interconversion to provide a better estimate of stable conformations. These results can be used to make future applications possible (Figure 1).

2. Methodology

Molecular modeling of the optimized eugenol and eugenyl acetate was carried out with the use of an efficient program for molecular mechanics (MM). Calculations are performed for all optimized geometries using AM1 and PM3 methods. The main molecular properties to characterize the geometry structures and the molecular orbital of the eugenyl acetate were calculated and compared. For each method, the geometry of the compound was optimized by using the Polak-Ribiere conjugate gradient algorithm with a gradient of 0.01 Kcal/mol (RMS). The following quantum chemical results are considered: heat of formation (ΔH_f), total energy (E_t), minimum energy of conformation ($E_{\text{min,conf}}$), strain energy of conformational interconversion (E_s), energy of highest occupied molecular orbital (HOMO), energy of lowest unoccupied molecular orbital (LUMO), and HOMO-LUMO energy gaps (EG).

3. Results and Discussion

Molecular geometries of eugenol and eugenyl acetate were optimized by semiempirical molecular orbital method (AM1

Table 1: Main calculated properties of eugenol and eugenyl acetate with semiempirical methods.

Entry	Properties	Eugenol							
		AM1				PM3			
		Trans	*Eclipsed*	*Gauche*	*Cis*	*Trans*	*Eclipsed*	*Gauche*	*Cis*
1	ΔH_f	−43.562	−45.560	−45.540	−38.360	−44.474	−45.230	−45.214	−40.236
2	E_t	−48090.984	−48092.980	−48092.960	−48085.781	−45111.215	−45111.973	−45111.957	−45106.976
3	$E_{\text{min,conf}}$	−2496.805	−2498.802	−2498.782	−2491.602	−2497.716	−2498.472	−2498.456	−2493.478
4	E_s	5.202	7.200	7.180	0.000	4.238	4.994	4.978	0.000
5	HOMO	−8.599	−8.614	−8.606	−8.592	−8.670	−8.703	−8.701	−8.666
6	LUMO	0.327	0.332	0.342	0.338	0.254	0.250	0.260	0.263
7	EG	8.926	8.946	8.948	8.930	8.924	8.953	8.961	8.929
Entry	Properties	Eugenyl acetate							
		AM1				PM3			
		Trans	*Eclipsed*	*Gauche*	*Cis*	*Trans*	*Eclipsed*	*Gauche*	*Cis*
8	ΔH_f	−68.176	−77.344	−77.356	−77.356	−77.728	−83.323	−83.330	−83.328
9	E_t	−62008.605	−62017.772	−62017.785	−62017.785	−58055.633	−58061.226	−58061.234	−58061.230
10	$E_{\text{min,conf}}$	−3026.961	−3036.129	−3036.140	−3036.140	−3036.514	−3042.108	−3042.115	−3042.113
11	E_s	9.180	0.012	0.000	0.000	5.600	0.005	−0.002	0.000
12	HOMO	−8.852	−9.215	−9.205	−9.205	−8.925	−9.302	−9.297	−9.299
13	LUMO	0.001	−0.134	−0.130	−0.130	−0.044	−0.191	−0.188	−0.189
14	EG	8.852	9.081	9.075	9.075	8.881	9.101	9.109	9.110

The strain energy (E_s) for each geometry of a molecule is defined as the difference between the minimum energy of conformation for that geometry and the most stable conformation of the molecule.

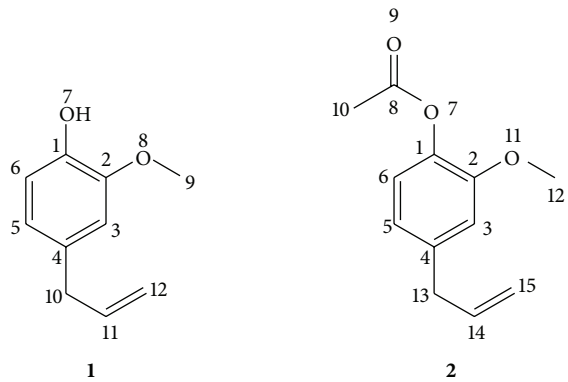

Figure 1: Conformation structures of *cis*-eugenol and *cis*-eugenyl acetate.

and PM3). The semiempirical simulations results for structure optimization of eugenol and eugenyl acetate are given in Table 1. The conformational interconversion energy-minimum of eugenyl acetate and eugenol was investigated in detail by changing different torsional angles. From these studies, we have determined five geometries of eugenol (three energy minima and two transition states) and three geometries of eugenyl acetate (two energy minima and one transition state). These geometries are important in the description of the conformational properties of our systems (Figure 2).

We have obtained the curves plotted in Figure 2 from the simulated data using the nonlinear fitting process based on the Levenberg-Marquardt algorithm implemented in the Origin v. 6.0. Software [20].

The dihedral angle for rotation about C_4–C_{10} bond in eugenol has several stationary points. A/A′, C, C′, and E/E′ are minima and B, B′ and D, D′ are maxima. Only the structures at the minima represent stable species and of these, the *syn* conformation is more stable than the *anti*. The *gauche* and the *eclipsed* represent the transition states. In eugenyl acetate, the stationary points A/A′, B/B′, C/C′, E/E′, F/F′, and G/G′ are minima and D, D′ are maxima. The *anti* conformation represents the transition state while the *syn*, *gauche*, and *eclipsed* conformations are stable species. So, the deformation around C_4–C_{13} in eugenyl acetate remains unchanged and is not influenced by torsional angle effect.

To provide a better estimate of conformations, we should search the conformational space in reasonable computing time. So, we run the simulations; then we run a geometry optimization on each structure. Thus, we have grouped the resulting structures in Figure 3. First, we observe that all geometries from *cis* conformations obtained after optimization present deformation mainly on branching allyl. The torsional angle value varies around 136°. This situation is due to methylene group (sp^3 hybridization) which gives a non-coplanar final geometry. Then, the π-bond of branching allyl is situated in the same side that acetate group. Second, we note that the geometry in *anti* conformations stays unchanged after optimization. All the substituents of aromatic ring, acetate and methoxy groups then branching allyl, are situated in the same plane (Φ*trans*: 180°).

From our molecular orbital calculations, we want to deduce the structure-reactivity relationship depending on different conformations. First, AM1 and PM3 calculations show that the *cis* forms are favored (Table 1, entry 7, EG: 9.075, 9.110 ev). On the other hand, the same calculations show that

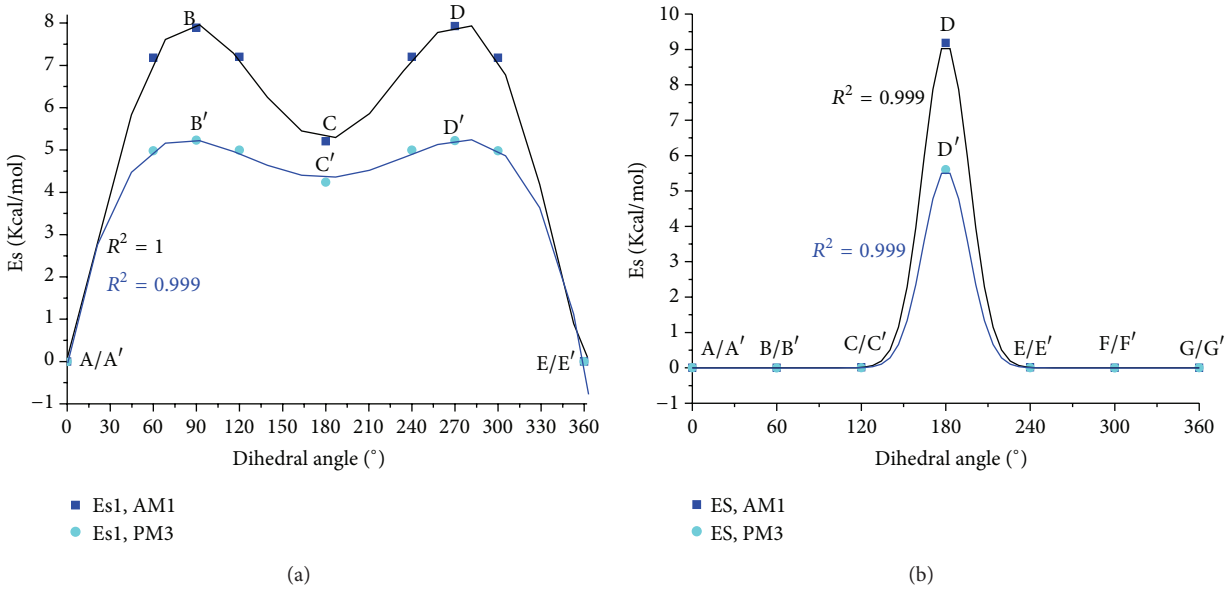

Figure 2: Calculated strain energy for conformational interconversion with semiempirical AM1 and PM3 methods. (a) Eugenol and (b) eugenyl acetate.

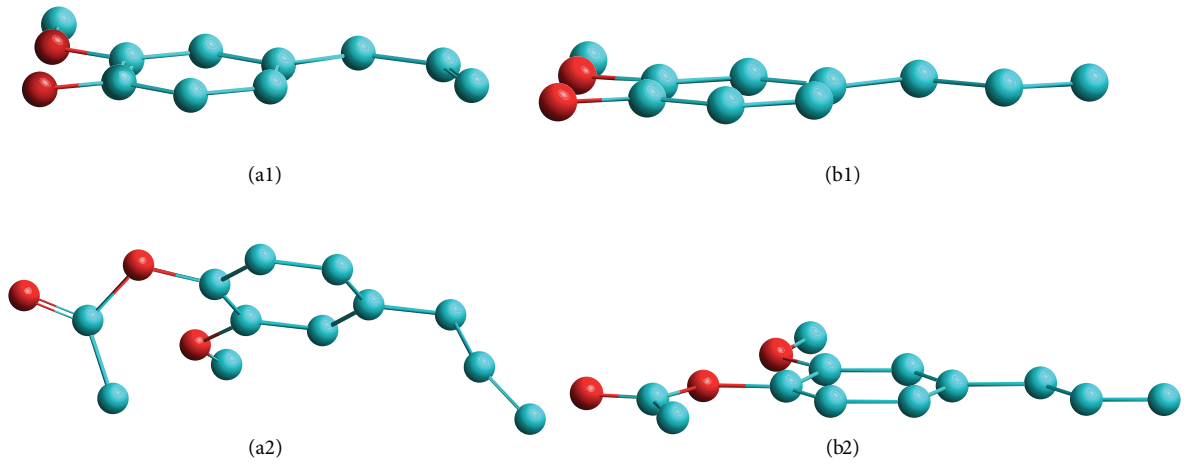

Figure 3: Estimated conformation structures of eugenol and eugenyl acetate; (a1) and (a2) *cis* forms, (b1) and (b2) *trans* forms. Molecule orientation was chosen around *x*-axis. Hydrogen atoms are omitted for clarity.

the most active site of the nucleophilic reaction is located on the oxygens of the acetate group and methoxy, and the most active site of the electrophilic reaction is C8 position of eugenyl acetate.

The AM1 and PM3 calculations show that the *trans* form is most active (Table 1, entry 7, EG: 8.852; 8.881 ev). Thus, these results reveal that the instability is caused by the high activity of methylene group in the strand allyl which provides to the aromatic ring another nucleophilic reaction site. This one is stabilized by resonance with the double bonds of the aromatic ring and the allylic radical (Figure 4). So, we note that the value of the strain energy obtained with AM1 method (Table 1, entry 4, Es: 9.180 ev) is higher than that obtained by PM3 calculation (Table 1, entry 4, Es: 5.600 ev). Consequently, we deduce that the optimized *trans* form by AM1 method is more reactive than under PM3 method. We can conclude that the efficient method for the eugenyl acetate is the semiempirical method AM1.

These observations remain the same for eugenol, except for the energy gaps. From Figure 2(a), we note that the *trans* form (C or C′) is near the transition states B and D, respectively, B′ and D′. This situation is clearer when the eugenol is optimized by PM3 (Table 1, entries 5 and 6, PM3: HOMO −8.599, LUMO 0.327 ev; AM1: HOMO −8.670, LUMO 0.254 ev). So, this *trans* form (C or C′) corresponds to the reaction intermediate present in eugenol and absent in eugenyl acetate (AM1: HOMO −8.606, LUMO 0.343; PM3: HOMO −8.702, LUMO 0.260 ev).

Furthermore, we also see that the HOMO is located at the oxygen sites whereas for the molecule the Homo is

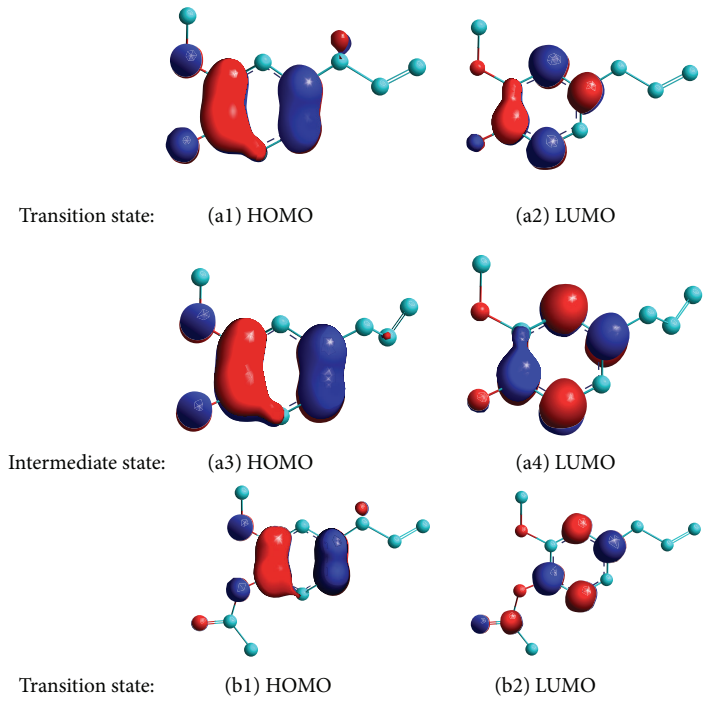

FIGURE 4: Molecular orbital calculated for eugenol and eugenyl acetate by semiempirical methods (AM1 and PM3). Contour values: 0.05 $Å^{-3}$. Blue lines represent positive contours. Red lines represent negative contours. Hydrogen atoms are omitted for clarity.

TABLE 2: Mulliken charges of the optimized structures of eugenol and eugenyl acetate.

Compound	State	Method	Type charge
Eugenol	Transition	AM1	C_1 0.065, C_2 0.058, C_3 −0.148, C_4 −0.078, C_5 −0.103, C_6 −0.165, O_7 −0.208, O_8 −0.166, C_9 0.047, C_{10} −0.019, C_{11} −0.134, C_{12} −0.168.
		PM3	C_1 0.063, C_2 0.063, C_3 −0.164, C_4 −0.072, C_5 −0.095, C_6 −0.169, O_7 −0.208, O_8 −0.166, C_9 0.047, C_{10} −0.017, C_{11} −0.143, C_{12} −0.170.
	Intermediate	AM1	C_1 0.054, C_2 0.058, C_3 −0.170, C_4 −0.067, C_5 −0.124, C_6 −0.185, O_7 −0.230, O_8 −0.187, C_9 0.079, C_{10} −0.096, C_{11} −0.156, C_{12} −0.224.
		PM3	C_1 0.065, C_2 0.058, C_3 −0.147, C_4 −0.078, C_5 −0.095, C_6 −0.169, O_7 −0.208, O_8 −0.166, C_9 0.047, C_{10} −0.019, C_{11} −0.134, C_{12} −0.168.
Eugenyl acetate	Transition	AM1	C_1 0.057, C_2 0.079, C_3 −0.197, C_4 −0.043, C_5 −0.136, C_6 −0.168, O_7 −0.190, C_8 0.306, O_9 −0.291, C_{10} −0.253, O_{11} −0.178, C_{12} −0.081, C_{13} −0.098, C_{14} −0.157, C_{15} −0.226.
		PM3	C_1 0.042, C_2 0.081, C_3 −0.174, C_4 −0.054, C_5 −0.113, C_6 −0.161, O_7 −0.156, C_8 0.351, O_9 −0.327, C_{10} −0.139, O_{11} −0.160, C_{12} 0.046, C_{13} −0.020, C_{14} −0.145, C_{15} −0.166.

distributed along the aromatic cycle site (Figure 4, Table 2). This clearly shows the high reactivity of eugenol compared to its corresponding acetate. This reactivity is due to mobility of hydrogen and the nucleophilicity on the aromatic ring.

From calculating wave functions, we observe that the charge distributions are mainly located on electrowithdrawing oxygen atoms in each molecule. They also are situated on aromatic ring and the strand allyl. The charge density is much higher under AM1 than under PM3. So, these results are in accordance with their energy properties (see Table 1) and the electronic properties of each substituent. The acetate group is an electron withdrawing type which reduces the aromatic cycle charge while hydroxyl group is an electron donor type that can provide its charge to the aromatic ring and thus increases its nucleophilic effect (Table 2).

4. Conclusion

In the present work, we have studied the conformational structure of eugenol and eugenyl acetate under torsional angle effect by performing semiempirical calculations using AM1 and PM3 methods. From quantum calculations, we have evaluated the strain energy of conformational interconversion. To provide a better estimate of stable conformations, we have plotted the strain energy versus dihedral angle. So,

we have determined five geometries of eugenol (three energy minima and two transition states) and three geometries of eugenyl acetate (two energy minima and one transition state). We have verified the presence of the intermediate form of eugenol which corresponds to the *trans* form (C or C′).

From the molecular orbital calculations, we deduce that the optimized *trans* form by AM1 method is more reactive than under PM3 method. We note that the charge distributions are mainly located on the aromatic ring and the strand allyl in each molecule. We can conclude that both methods are efficient. The AM1 method allows us to determine the reactivity and PM3 method to verify the stability.

Conflict of Interests

The author declares that there is no conflict of interest regarding the publication of this paper.

References

[1] E. Reverchon, "Supercritical fluid extraction and fractionation of essential oils and related products," *The Journal of Supercritical Fluids*, vol. 10, no. 1, pp. 1–37, 1997.

[2] W. Guan, S. Li, R. Yan, S. Tang, and C. Quan, "Comparison of essential oils of clove buds extracted with supercritical carbon dioxide and other three traditional extraction methods," *Food Chemistry*, vol. 101, no. 4, pp. 1558–1564, 2007.

[3] M. N. I. Bhuiyan, J. Begum, N. C. Nandi, and F. Akter, "Constituents of the essential oil from leaves and buds of clove (*Syzygium caryophyllatum* (L.) Alston)," *African Journal of Plant Science*, vol. 4, pp. 451–454, 2010.

[4] S. M. Palacios, A. Bertoni, Y. Rossi, R. Santander, and A. Urzúa, "Efficacy of essential oils from edible plants as insecticides against the house fly, *Musca domestica* L," *Molecules*, vol. 14, no. 5, pp. 1938–1947, 2009.

[5] M. H. Alma, M. Ertaş, S. Nitz, and H. Kollmannsberger, "Chemical composition and content of essential oil from the bud of cultivated Turkish clove (*Syzygium aromaticum* L.)," *BioResources*, vol. 2, no. 2, pp. 265–269, 2007.

[6] A. K. Srivastava, S. K. Srivastava, and K. V. Syamsundar, "Bud and leaf essential oil composition of *Syzygium aromaticum* from India and Madagascar," *Flavour and Fragrance Journal*, vol. 20, no. 1, pp. 51–53, 2005.

[7] K.-G. Lee and T. Shibamoto, "Antioxidant property of aroma extract isolated from clove buds [*Syzygium aromaticum* (L.) Merr. et Perry]," *Food Chemistry*, vol. 74, no. 4, pp. 443–448, 2001.

[8] A. A. Clifford, A. Basile, and S. H. R. Al-Saidi, "A comparison of the extraction of clove buds with supercritical carbon dioxide and superheated water," *Fresenius' Journal of Analytical Chemistry*, vol. 364, no. 7, pp. 635–637, 1999.

[9] G. Della Porta, R. Taddeo, E. D'Urso, and E. Reverchon, "Isolation of clove bud and star anise essential oil by supercritical CO_2 extraction," *LWT—Food Science and Technology*, vol. 31, no. 5, pp. 454–460, 1998.

[10] F. N. Lugemwa, "Extraction of betulin, trimyristin, eugenol and carnosic acid using water-organic solvent mixtures," *Molecules*, vol. 17, no. 8, pp. 9274–9282, 2012.

[11] B. Jayawardena and R. M. Smith, "Superheated water extraction of essential oils from *Cinnamomum zeylanicum* (L.)," *Phytochemical Analysis*, vol. 21, no. 5, pp. 470–472, 2010.

[12] S. Ghosh, D. Chatterjee, S. Das, and P. Bhattacharjee, "Supercritical carbon dioxide extraction of eugenol-rich fraction from Ocimum sanctum Linn and a comparative evaluation with other extraction techniques: process optimization and phytochemical characterization," *Industrial Crops and Products*, vol. 47, pp. 78–85, 2013.

[13] S. Ghosh, D. Roy, D. Chatterjee, P. Bhattacharjee, and S. Das, "SFE as a superior technique for extraction of eugenol-rich fraction from *Cinnamomum tamala* Nees (Bay Leaf)-process analysis and phytochemical characterization," *International Journal of Biological, Life Science and Engineering*, vol. 8, no. 1, pp. 9–17, 2014.

[14] F. Memmou and R. Mahboub, "Composition of essential oil from fresh flower of clove," *Journal of Scientific Research in Pharmacy*, vol. 1, pp. 33–35, 2012.

[15] M. He, M. Du, M. Fan, and Z. Bian, "In vitro activity of eugenol against Candida albicans biofilms," *Mycopathologia*, vol. 163, no. 3, pp. 137–143, 2007.

[16] S. A. Guenette, F. Beaudry, J. F. Marier, and P. Vachon, "Pharmacokinetics and anesthetic activity of eugenol in male Sprague-Dawley rats," *Journal of Veterinary Pharmacology and Therapeutics*, vol. 29, no. 4, pp. 265–270, 2006.

[17] G. Blank, A. A. Adejumo, and J. Zawistowski, "Eugenol induced changes in the fatty acid content two *Lactobacillus* species," *Lebensmittel-Wissenschaft. Technology*, vol. 24, pp. 231–235, 1991.

[18] A. L. Dos Santos, G. O. Chierice, K. Alexander, and A. Riga, "Crystal structure determination for eugenyl acetate," *Journal of Chemical Crystallography*, vol. 39, no. 9, pp. 655–661, 2009.

[19] A. L. Dos Santos, G. O. Chierice, A. T. Riga, K. Alexander, and E. Matthews, "Thermal behavior and structural properites of plant-derived eugenyl acetate," *Journal of Thermal Analysis and Calorimetry*, vol. 97, no. 1, pp. 329–332, 2009.

[20] D. W. Marquardt, "An algorithm for least-squares estimation of nonlinear parameters," vol. 11, pp. 431–441, 1963.